Microelectronic Engineering 87 (2010) 715–718

Contents lists available at ScienceDirect

Microelectronic Engineering

journal homepage: www.elsevier.com/locate/mee

Bacterial adhesion to toroidal nano-structures from poly(styrene)-*block*-poly(*tert*-butyl acrylate) diblock copolymer thin films

Shuyan Li [a], Andras Z. Komaromy [a], Dan V. Nicolau [a,b], Reinhard I. Boysen [a,*], Milton T.W. Hearn [a]

[a] ARC Special Research Centre for Green Chemistry, Monash University, Clayton, VIC 3800, Australia
[b] Department of Electrical Engineering and Electronics, The University of Liverpool, Brownlow Hill, Liverpool L69 3GJ, UK

ARTICLE INFO

Article history:
Received 14 September 2009
Received in revised form 4 December 2009
Accepted 9 December 2009
Available online 16 December 2009

Keywords:
Diblock copolymer
Thin film
Self-assembly
Toroids
Bacterial adhesion
Staphylococcus aureus
Cell viability

ABSTRACT

Nano-structured thin films with protruding P*t*BA nanodomain structures were obtained from the deposition, spin-coating, self-assembly and annealing of the diblock copolymer poly(styrene)-*block*-poly(*tert*-butyl acrylate) (PS-*b*-P*t*BA). The topography has been documented by atomic force microscopy. The sacrificial removal of the P*t*BA block from these thin film structures after UV irradiation yielded surfaces with 5/7 segmented polystyrene (PS) toroids of 100–150 nm diameter. These polymeric materials (as well as the corresponding homopolymeric materials derived from PS and P*t*BA) were incubated with *Staphylococcus aureus* cells. Live and dead cell numbers were determined in replicate trials by fluorescence microscopy after the cells were stained for viability. *S. aureus* formed colonies of 5–200 cells on the nanodomain and toroid-containing surfaces as assessed by AFM, but only attached sparsely as single cells onto a planar P*t*BA surface. Cell viability and adhesion was found to be influenced by a combined effect of the surface hydrophilicity and topography. The results demonstrate a synthetic route to produce polymeric surfaces with nano-toroids which are capable of modifying bacterial adhesion.

1. Introduction

Self-assembling polymers spontaneously form highly ordered nano-structures and provide simple, parallel, and cost-effective processes for nanofabrication. Self-assembly of block co-polymers can be used to create a variety of thin film surface topographies like spheres, cylinders, squares, lamellae and gyroids [1]. The structure of the polymeric thin films can be affected by the choice of solvent at the spin-coating stage or temperature during the annealing process. Blocks can further be chemically modified to permit protein immobilization [2]. In the last decade, polymer thin films have received increasing interest since they can be used to modify cellular adhesion [3–6]. Moreover, they can be made to combine topographical patterning with nanometre scale precision and the possibility of robust (bio)functionalization with controlled molecular loading [7]. The poly(styrene)-*block*-poly(*tert*-butyl acrylate) (PS-*b*-P*t*BA) diblock copolymer [8,9] possesses these characteristics. The self-assembly of this system into microphase separated topographical elements allows the generation of sub-100 nm structures, therefore creating structures matching the typical spacing between proteins, protein clusters and other biomolecules on the surface of cells or cell aggregates. Although this PS-*b*-P*t*BA system has been applied in the past to modify the adhesion of relatively large mammalian cells up to 10 μm in diameter [10], it had not been explored for small pathogenic bacteria like *Staphylococcus aureus*, which typically have a diameter of 500 nm. In an earlier study [11], we have demonstrated that block copolymer microstructures can be generated to achieve either bacterial adhesion or repellence. In the present investigation, PS-*b*-P*t*BA was chosen to explore the effect of the sacrificial removal of the P*t*BA block on the thin film structure and the properties of the derived materials with respect to bacterial responses.

2. Methodology

2.1. Synthesis of the thin film polymer

The PS_n-*b*-$PtBA_m$ diblock copolymer with the block molecular weight (repeat units $n_1 = 432$, $m_1 = 250$, where n_i and m_i correspond to the degree of polymerization of the respective blocks in the block co-polymers) was purchased from Polymer Source Co. (Dorval, Canada). The molecular weight of the parent polymer was 66.2 kg mol^{-1}, that of P*t*BA was 32.0 kg mol^{-1}. The polydispersity index was 1.05. Monohydroxyl terminated polystyrene (PS-OH) (MW 100,000) was purchased from Scientific Polymer Products Inc. (Ontario, New York, USA). Polymer thin films were produced starting from clean silicon wafers possessing a natural oxidized layer. The wafers were covered by a PS polymer brush using spin-coating [12]. Thereafter, the diblock copolymer solution

* Corresponding author. Tel.: +61 3 9905 4516; fax: +61 3 9905 8501.
E-mail address: reinhard.boysen@sci.monash.edu.au (R.I. Boysen).

0167-9317/$ - see front matter © 2010 Elsevier B.V. All rights reserved.
doi:10.1016/j.mee.2009.12.042

in toluene (1–2 wt.%) was spin coated onto the silicon wafers at 2000–4000 rpm for 1 min using a wafer spin processor (Laurell Technologies Corporation, North Wales, USA). The thickness of the film was controlled to be approximately 40 nm by the concentration of the polymer in the solution and the spinning speed. All spin-cast samples were annealed at 130 °C for 2 days, thereafter for 1 day at 160 °C in a vacuum before initial atomic force microscopy (AFM) analysis. The P*t*BA block chains were then selectively removed by UV exposure for 10–30 s (UV-TipCleaner, Bioforce Nanosciences Inc. Ames, USA) and acetic acid washing [13]. Preparation of the reference surfaces on silicon wafers (unmodified silicon, gold, hydrophilic or hydrophobic self-assembled monolayer) was achieved as described in [11].

2.2. Thermogravimetric analysis

Thermogravimetric analysis (TGA) was performed to assess polymer stability. The isothermal weight loss over time of 10 mg PS_{432}-*b*-P*t*BA_{250} bulk polymer samples under nitrogen was measured at 160 °C. Dynamic TGA was performed with heating over the temperature range of 30–300 °C at a rate of 10 °C/min with a Perkin–Elmer thermogravimetric analyzer (TGA 7, Waltham, MA) using a constant nitrogen flow of 30 mL/min.

2.3. Bacterial cell culture

S. aureus (ATCC 6538) was obtained from the Department of Microbiology, Monash University, Melbourne, Australia, and grown in 2YT medium. One litre 2YT medium contained 16 g tryptone, 10 g yeast extract and 5 g NaCl. The pH was adjusted to 7.2. Cells were grown until they reached the mid-log phase, centrifuged and the pellets resuspended in phosphate buffer to adjust the final cell concentration to $1–3 \times 10^8$ colony forming units/mL. All wafers with thin film polymers were incubated in the cell suspensions for two hours, washed twice with phosphate buffer and ultra pure water and air-dried at room temperature.

2.4. Fluorescence staining and microscopy

The thin film polymers, after having been incubated with the bacterial solutions, were soaked in a solution of live/dead *BacLight* bacterial viability fluorescent dye (Invitrogen Pty Ltd., Melbourne, Australia) for 15 min and washed with sterile ultra pure water, dried and investigated with an Olympus BX51 fluorescence microscope (Olympus Corporation, Tokyo, Japan) in the reflectance mode. Images were taken in fluorescence mode using a U-MWB2 cube for live and a U-MWG2 cube for dead cells or in the differential interference contrast (DIC) mode with a digital Spot R3 camera (Diagnostic instruments, Inc., Sterling Heights, MI, USA). Image and data processing were carried out with the Image-Pro Plus 6.0 software (Media Cybernetics, Inc. Silver Spring, MD, USA) to count the numbers of live and dead bacteria in triplicate measurements.

2.5. Contact angle measurements

Static contact angles of all surfaces (planar reference surfaces as well as thin film polymer surfaces) were measured with an OCA 20 contact angle goniometer (Dataphysics Instruments GmbH, Filderstadt, Germany) using the sessile drop technique with 1 μL of ultra pure water ($18.2\ \Omega\ cm^{-1}$) in air at room temperature (20–23 °C).

2.6. Surface analysis

Surface characterization was undertaken with a PicoPlus atomic force microscope (AFM) interfaced with a Picoscan 3000 controller (both from Molecular Imaging Inc., USA). A silicon cantilever (Ultrasharp, NSC15/AIBS, MikroMasch) was used with a typical spring constant of 40 N/m in tapping mode. The resulting images were analyzed using software WS×M 4.0 Develop 10.4.

3. Results and discussion

The PS_{432}-*b*-P*t*BA_{250} diblock copolymer, deposited onto the silicon wafer substrates (previously neutralized with a PS brush) via a spin-coating procedure, resulted in thin films of controlled thickness (<40 nm). After annealing, the nano-topography was investigated with atomic force microscopy (AFM). A thin film with protruding P*t*BA nanodomains with an average diameter of 43.74 nm (STD 0.71 nm) due to a microphase separation was obtained (Fig. 1). The formation of these nanodomains is consistent with the lower surface tension of P*t*BA compared to that of PS (γ_{PtBA} = 31.2 mN/m; γ_{PS} = 40.7 mN/m). Dynamic TGA data of bulk PS-*b*-P*t*BA showed that thermolysis only occurred at temperatures above 215 °C with 16.16% weight loss, whilst isothermal TGA data of bulk PS-*b*-P*t*BA samples at 160 °C for 720 min further confirmed the stability of this polymer under these conditions. Upon removal of the P*t*BA nanodomains by ultraviolet irradiation and acetic acid treatment, AFM revealed a thin film surface with segmented PS

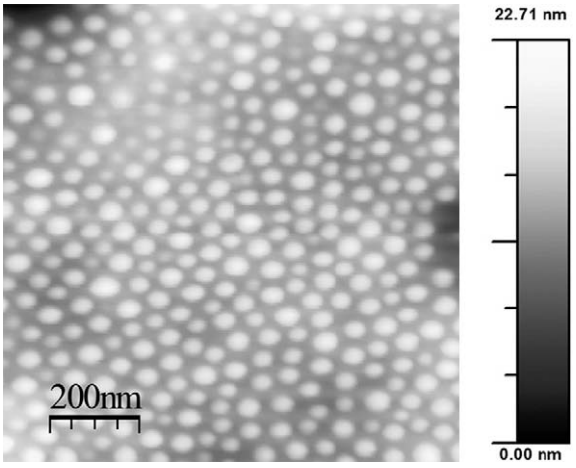

Fig. 1. AFM image of the nano-topography of a PS_{432}-*b*-P*t*BA_{250} thin film after annealing showing protruding P*t*BA nanodomains of 35–50 nm diameter.

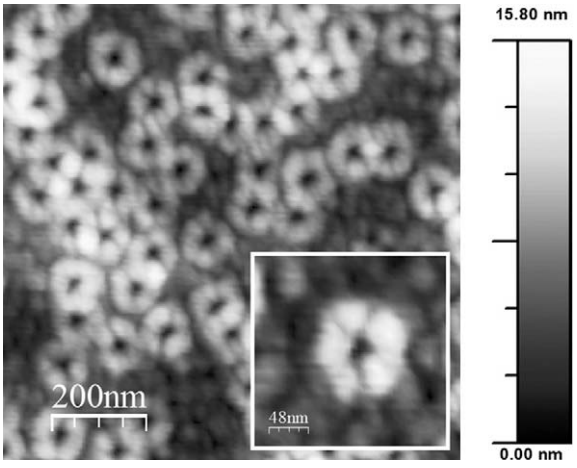

Fig. 2. AFM image of the nano-topography of a PS_{432}-*b*-P*t*BA_{250} thin film subjected to UV-etching and acetic acid washing. (Inset) Single segmented toroidal PS structure consisting of five subunits around the void created by the sacrificed P*t*BA.

Table 1
Contact angles of the homopolymer and diblock copolymer thin films as well as reference surfaces and associated cell counts.

	Surface	Contact angle θ (°)	Live cells (SD)/100 μm^2
Planar surfaces	Unmodified silicon	14 ± 3	1.47 (1.51)
	Hydrophilic SAM	14 ± 2	0.53 (0.41)
	Gold	35 ± 5	2.12 (0.85)
	PS after UV irradiation	69.4 ± 0.8	n.d.
	P*t*BA	84.7 ± 0.6	0.5 (0.2)
	PS_{432}-*b*-P*t*BA_{250}	85.9 ± 1.1	n.d.
	PS	86.9 ± 0.7	0.1 (0.0)
	Hydrophobic SAM	105 ± 3	0.04 (0.4)
Nano-structured surfaces	PS_{432}-*b*-P*t*BA_{250} after annealing	90.5 ± 0.2	3.6 (0.3)
	PS_{432}-*b*-P*t*BA_{250} after annealing and UV-etching	72.7 ± 0.4	5.8 (0.2)

toroids of predominantly five subunits (with some toroids of tetra- and hexa-symmetry) (Fig. 2). The toroids were of 100–120 nm diameter with average diameters of the central toroid voids of 22.75 nm.

To assess the propensity of bacterial cells to adhere to these structured thin film polymer surfaces, these new materials as well as the planar films of PS and P*t*BA and other reference planar surfaces were incubated for 2 h with suspensions of *S. aureus*. The number of live and dead bacterial cells was counted in replicate trials, with bacterial attachment imaged by fluorescence microscopy in the reflectance mode.

The cell viability studies with the planar surfaces revealed (Table 1) that live *S. aureus* preferentially attached to hydrophilic planar surfaces (e.g., gold $\theta = 35 \pm 5°$), but not to extremely hydrophilic surfaces (like hydrophilic SAM coated gold $\theta = 14 \pm 2°$) nor to hydrophobic planar surfaces (P*t*BA $\theta = 84.7 \pm 0.6°$, PS $\theta = 86.9 \pm 0.7°$, hydrophobic SAM $\theta = 105 \pm 3°$). The comparison of cellular adhesion to smooth surfaces (surfaces roughness <5 nm) shows that *S. aureus*, in the absence of chemical surface modifications or shear forces, prefers moderately hydrophilic surfaces under physiological conditions. Bacterial counts (Fig. 3) on nano-structured surfaces showed that live *S. aureus* significantly preferred toroidal structures (5.8 ± 0.2 cells/100 μm^2) compared to nanodomains (3.6 ± 0.2 cells/100 μm^2) and discriminated against flat PS (0.1 cells/100 μm^2) or P*t*BA surfaces (0.5 live cells/100 μm^2). The cell count on nano-structured thin films with protruding P*t*BA nanodomains exceeded that of planar structures with similar hydrophobicity by seven fold. When these films were exposed to UV to deplete the P*t*BA component, the remaining polystyrene toroidal surface becomes more hydrophilic than the planar polystyrene which may explain the higher cell count. The bacterial adhesion with these PS toroidal surfaces was even higher than that of the hydrophilic gold which showed the highest bacterial adherence of the planar surfaces. Thus, the nanostructuring of a favourable (hydrophilic) surface can lead to an enhancement of the adhesion of *S. aureus* which may be a direct result of the increased area for the cell–surface interaction. A similar effect was observed for the interaction of *S. aureus* with a nano-array of grooved surfaces, where the highest *S. aureus* cell count was obtained for surfaces with grooves width dimensionally larger than the individual bacterial cells, thus allowing cellular insertion, again maximising the bacteria-surface contact area [14].

When the surfaces were analyzed with AFM, *S. aureus* was shown to form colonies on both the toroid- (Fig. 4) and nanodomain- (Fig. 5) containing surfaces; however this occurred less densely, mainly as single cells on a planar P*t*BA surface (inset in Fig. 4). Moreover, *S. aureus* generated extra-cellular substances, which extended out onto both of the nano-structured surfaces (Fig. 4), but did not occur on a hydrophilic glass surface. The generation of the extra-cellular substance biofilm may enable bacterial growth

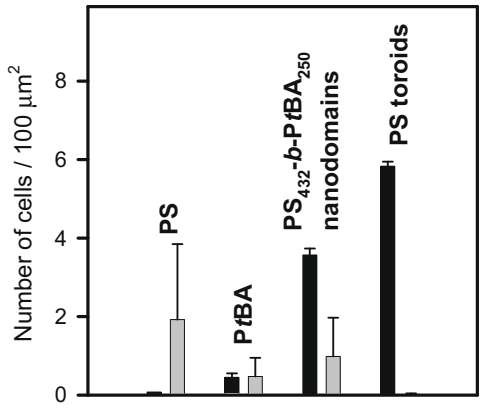

Fig. 3. Number of adhered live (black) and dead (grey) *S. aureus* cells/100 μm^2 on PS and P*t*BA homopolymers thin films as well as the PS-*b*-P*t*BA diblock copolymer thin films after annealing and after UV-etching.

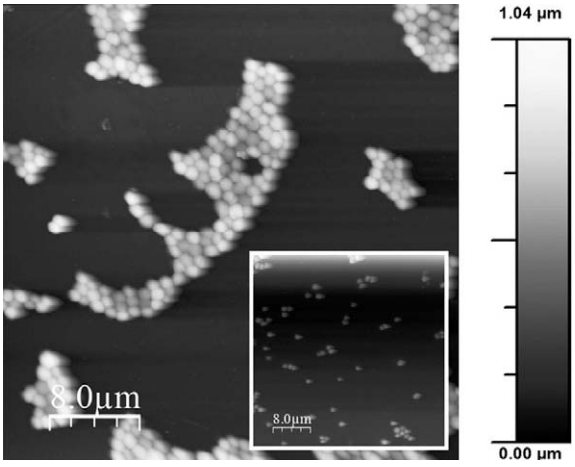

Fig. 4. AFM image of colonies of *Staphylococcus aureus* cells attached to the nano-structured thin film with toroids as in Fig. 2. (Inset) *S. aureus* cells on a planar P*t*BA surface.

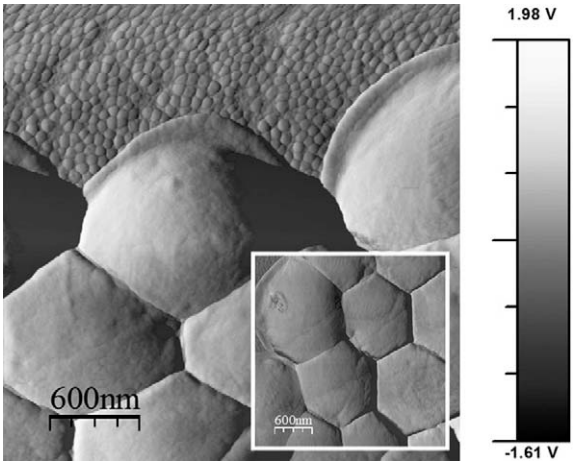

Fig. 5. AFM phase image of *S. aureus* cells attached to the nano-structured PS$_{432}$-*b*-P*t*BA$_{250}$ thin film with nanodomains as in Fig. 1. (Inset) *S. aureus* cells attached to nano-structured thin film as in Fig. 2 and 4. On both surfaces extra-cellular substance anchors the bacteria.

on structured surfaces which are sub-optimal in terms of surface hydrophobicity.

4. Conclusion

The results demonstrate a new approach to prepare polymeric thin film surfaces containing toroidal nano-structures, derived from PS-*b*-P*t*BA. These thin film surfaces exhibit a higher adhesion of *S. aureus* cells compared to the PS-*b*-P*t*BA thin films with nanodomains, i.e. films containing both block co-polymers. With these latter polymeric thin films with nanodomains adhesion of *S. aureus* cells occurs despite a surface hydrophobicity which is higher than that of the homopolymeric planar P*t*BA and PS reference surfaces where very low bacterial attachment was detected. Similar results were obtained for *Streptococcus agalactiae* and further investigations on other bacteria will be undertaken. These nano-structures could find applications as adhesive lawns for beneficial microorganisms in the food or aroma industry and may be tools to investigate the mechanisms of adhesion and biofilm formation of microbial organisms.

Acknowledgements

This Project is supported by the Commonwealth of Australia under the International Science Linkages program. This research was supported by the European–Australian integrated FP6 project CHARPAN and FP7 project BISNES.

References

[1] T. Smart, H. Lomas, M. Massignani, M.V. Flores-Merino, L.R. Perez, G. Battaglia, Nano Today 3 (2008) 38–46.
[2] C.L. Feng, G.J. Vancso, H. Schoenherr, Langmuir 21 (2005) 2356–2363.
[3] G. Speranza, G. Gottardi, C. Pederzolli, L. Lunelli, R. Canteri, L. Pasquardini, E. Carli, A. Lui, D. Maniglio, M. Brugnara, M. Anderle, Biomaterials 25 (2004) 2029–2037.
[4] P. Kim, D.H. Kim, B. Kim, S.K. Choi, S.H. Lee, A. Khademhosseini, R. Langer, K.Y. Suh, Nanotechnology 16 (2005) 2420–2426.
[5] I.Y. Tsai, M. Kimura, T.P. Russell, Langmuir 20 (2004) 5952–5957.
[6] J.P. Spatz, B. Geiger, Methods Cell Biol 83 (2007) 89–111.
[7] J. Duvigneau, H. Schoenherr, G.J. Vancso, Langmuir 24 (2008) 10825–10832.
[8] A. Embrechts, C.L. Feng, C.A. Mills, M. Lee, I. Bredebusch, J. Schnekenburger, W. Domschke, G.J. Vancso, H. Schoenherr, Langmuir 24 (2008) 8841–8849.
[9] D.-H. Park, Nanotechnology 18 (2007) 365303/1–365303/6.
[10] C.L. Feng, A. Embrechts, I. Bredebusch, A. Bouma, J. Schnekenburger, M. Garcia-Parajo, W. Domschke, G.J. Vancso, H. Schoenherr, Eur. Polym. J. 43 (2007) 2177–2190.
[11] A. Komaromy, R.I. Boysen, H. Zhang, I. McKinnon, F. Fulga, M.T.W. Hearn, D.V. Nicolau, Microelectron. Eng. 86 (2009) 1431–1434.
[12] P. Mansky, Y. Liu, E. Huang, T.P. Russell, C. Hawker, Science 275 (1997) 1458–1460.
[13] Y.-H. La, E.W. Edwards, S.-M. Park, P.F. Nealey, Nano Lett. 5 (2005) 1379–1384.
[14] A. Komaromy, R.I. Boysen, H. Zhang, M.T.W. Hearn, D.V. Nicolau, in: Proc. SPIE 7270 Biomedical Applications of Micro- and Nanoengineering IV and Complex Systems, 2008, pp. 727006/1–727006/8.